

LA-UR-21-32382

Approved for public release; distribution is unlimited.

Title: Beam Coupling Impedances of Inter-cell Section in Scorpion Linac

Author(s): Kurennoy, Sergey S.

Intended for: Distribution to external collaborators

Issued: 2021-12-20



Los Alamos National Laboratory, an affirmative action/equal opportunity employer, is operated by Triad National Security, LLC for the National Nuclear Security Administration of U.S. Department of Energy under contract 89233218CNA000001. By approving this article, the publisher recognizes that the U.S. Government retains nonexclusive, royalty-free license to publish or reproduce the published form of this contribution, or to allow others to do so, for U.S. Government purposes. Los Alamos National Laboratory requests that the publisher identify this article as work performed under the auspices of the U.S. Department of Energy. Los Alamos National Laboratory strongly supports academic freedom and a researcher's right to publish; as an institution, however, the Laboratory does not endorse the viewpoint of a publication or guarantee its technical correctness.

Abstract

The following technical note is prepared for distribution to external project collaborators.

An inter-cell pumping section in the Scorpius linac contains a pumping grid with slots, bellows, and vacuum plenum. The beam coupling impedances of the inter-cell section are calculated with CST Studio.

Important to note that all impedance values in the tech note below should be divided by a factor of 2 to obtain the beam coupling impedances in their standard definition; see reference¹ for details.

¹ S.S. Kurennoy, R.C. McCrady. "Beam Coupling Impedances of Ferrite-Loaded Cavities: Calculations and Measurements." LA-UR-21-25475, Los Alamos, 2021; IPAC21, Campinas, SP, Brazil, 2021, pp. 696-8.



Technical Note

Accelerator Operation and Technology

AOT-AE Group:

Accelerators & Electrodynamics

To/MS: Distribution

From/MS: Sergey Kurennoy, AOT-AE / H817

Phone/Fax: 505-665-1459 / 505-667-8207

E-mail: kurennoy@lanl.gov

Symbol: AOT-AE: 20-009 (TN)

Date: August 31, 2020

SUBJECT: Coupling impedances of inter-cell section in Scorpius linac.

An inter-cell pumping section in the Scorpius linac contains a pumping grid with slots, bellows, and vacuum plenum. The beam coupling impedances of the inter-cell section are calculated with CST Studio.

Distribution:

AOT-AE			(e-mail copy)
E. Colunga	ASD-TECH	MS H816	(e-mail copy)
M.T. Crawford	ASD-TECH	MS H816	(e-mail copy)
C.A. Ekdahl Jr.	J-5	MS P912	(e-mail copy)
A.K. Ortega	ASD-TECH	MS H816	(e-mail copy)
J.M. Taccetti	J-5	MS P912	(e-mail copy)

1. Introduction.

A vacuum chamber of any accelerator contains multiple small discontinuities such as pumping holes, connections between smooth pieces of beam pipe, etc. These discontinuities contribute to the beam coupling impedances, and it is important to make sure that these impedances are acceptable from the viewpoint of beam stability. A general analytical method for calculating the impedances of small discontinuities was developed in [1]. The beam coupling impedances due to small discontinuities are inductive at low frequencies, i.e. frequencies well below the beam-pipe cutoff. Small discontinuities can create trapped modes near the cutoff; they also produce some high-frequency resonances well above the cutoff, at frequencies inversely proportional to characteristic dimensions of discontinuity.

The inter-cell section of an induction linac represents a combination of small discontinuities (pumping slots, bellows) with a large asymmetric resonator (vacuum plenum) that is coupled to the beam pipe by slots. The impedances of some elements were analyzed previously [2, 3], but since then the inter-cell design changed. We use CST Studio [4] to calculate the beam coupling impedances for the new design of the inter-cell pumping section.

2. Vacuum plenum.

2.1. Layout. A simplified CST model of inter-cell section is shown in Fig. 1. A vacuum plenum consists of a duct that is attached to a short cylinder surrounding a stainless-steel grid with pumping slots. The beam pipe and pumping grid both have ID 5.834" (inner radius $b = 74.0918$ mm) and OD 6"; the grid thickness is 2.1082 mm. The CST model was assembled using imported details from CAD files [5] and additional simple shapes created in the CST modeler, to keep essential features but make it simple enough for calculations. The inner bellows, near the grid, were created in CST. The outer bellows, near the flange on the cylinder wall that surrounds the grid, are replaced by a simple small cavity. Their exact shape is not important since they are not exposed to the beam fields directly. Next to the inner bellows, there is a small annular gap due to module connection; it is 2-mm wide and 5-mm deep, see in Fig. 1 (right). The beam pipe, grid, bellows, and plenum walls are made of stainless steel.

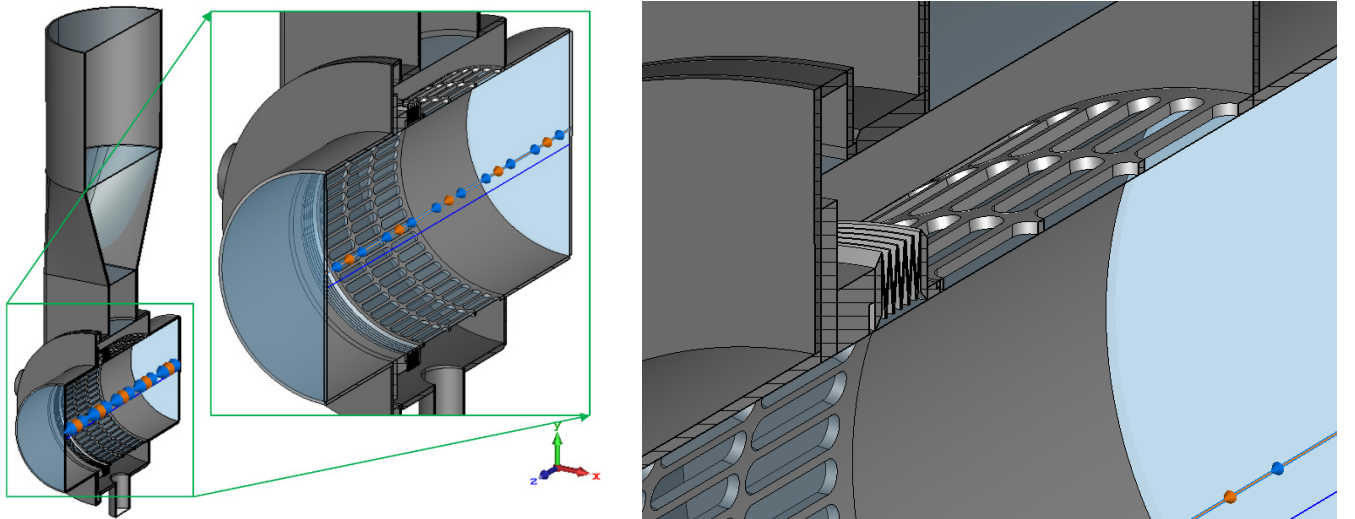


Figure 1: CST model of the inter-cell section: beam pipe, grid with pumping slots, bellows, and vacuum plenum (gray); vacuum volume is shown in transparent blue; enlarged cut view at $x = 0$ (right).

The vacuum plenum starts as a cylindrical extension that surrounds the pumping grid. It is connected to a duct of rectangular cross section with dimensions 3" x 8". The duct is connected via transition section to a wide cylindrical pipe, which will be connected to a vacuum pump. The section is inserted between two linac cells, so there are other elements located nearby, but for our purposes, it is sufficient to consider the inter-cell section as one combined discontinuity on a uniform beam pipe.

2.2. Coupling impedances from wake potentials. The cutoff frequencies for the beam pipe of inner radius $b = 74.0918$ mm are $f_h = 1185.68$ MHz for TE_{11} (H-modes) and $f_e = 1548.65$ MHz for TM_{01} (E-modes). We use CST wake-field solver to calculate wake potentials due to a Gaussian linear charge distribution with $\sigma_z = 25$ mm passing through the inter-cell section up to the distance of $s = 25$ m behind the bunch. The bunch path was taken on the beam axis ($x = y = 0$) for the longitudinal wake and offset transversely from the axis by distance d , either vertically ($y = d$) or horizontally ($x = d$), for the transverse wake, with proper boundary conditions. The resulting longitudinal coupling impedance is plotted in Fig. 2. One can see that the impedance is inductive and its real part is negligible up to the cutoff frequency, cf. [2, 3]. The first resonance is near the E-mode cutoff; it is rather weakly excited.

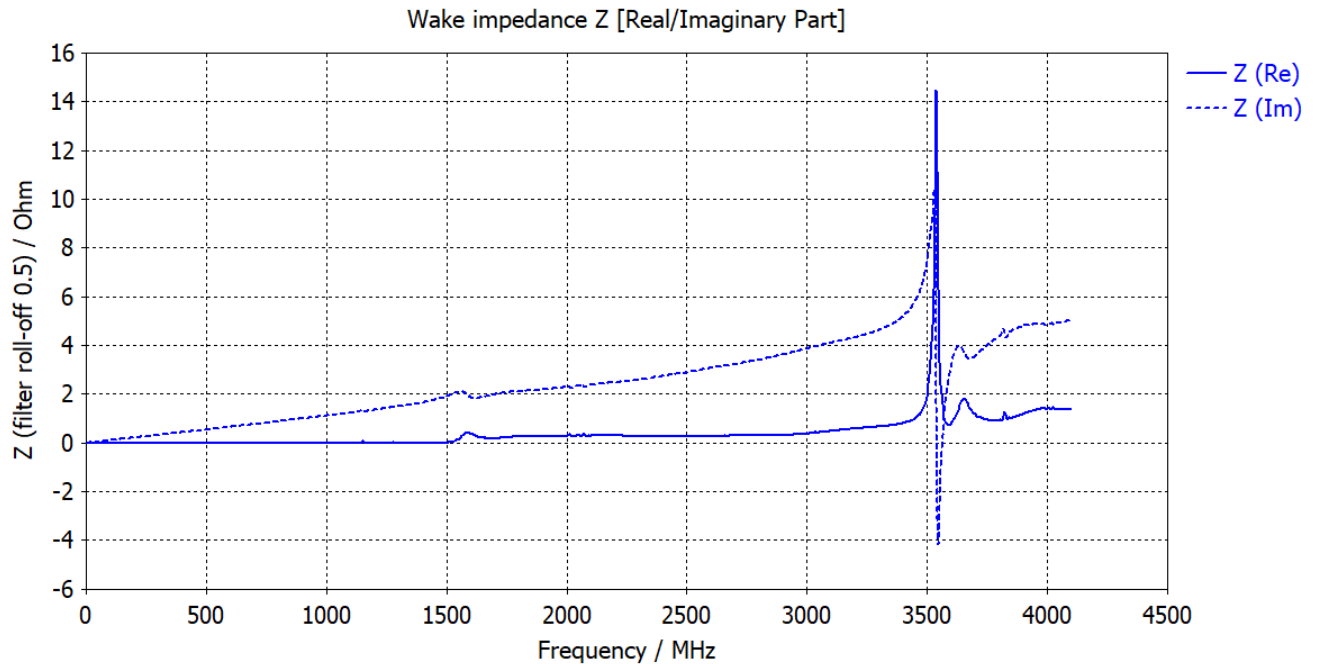


Figure 2: The longitudinal coupling impedance (solid curve – real part, dashed – imaginary part) of the inter-cell section, calculated from wake potentials, versus frequency.

The inter-cell section is symmetric in the horizontal direction, i.e. w.r.t. the plane $x = 0$. This means that the horizontal transverse dipole coupling impedance can be calculated directly in CST post-processing, see in [3]; it is plotted in Fig. 3. The imaginary part of the horizontal transverse impedance in Fig. 3 is nearly constant, about $37 \Omega/\text{m}$, while the real part is close to zero, in the frequency range up to 1 GHz. The lowest resonances are around 1.2 GHz, near the H-mode cutoff.

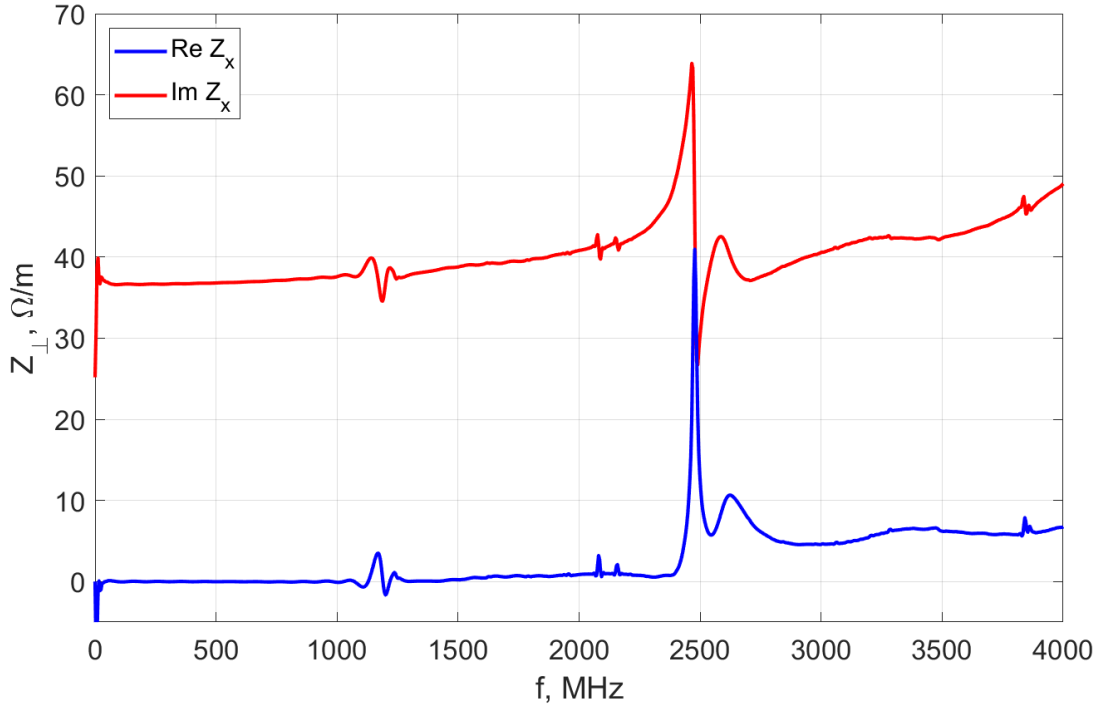


Figure 3: The horizontal dipole impedance (blue – real part, red – imaginary part) of the inter-cell section, calculated from wake potentials, versus frequency.

In the vertical direction, the inter-cell section is asymmetric, so we need two CST runs with different vertical transverse offsets, d_1 and d_2 , to exclude other terms in calculating the transverse vertical dipole coupling impedance [3]:

$$Z_{\perp y} = \frac{Z_{\perp y}(d_2)d_2 - Z_{\perp y}(d_1)d_1}{d_2 - d_1}. \quad (1)$$

The results for the real part of the vertical impedance are illustrated in Fig. 4.

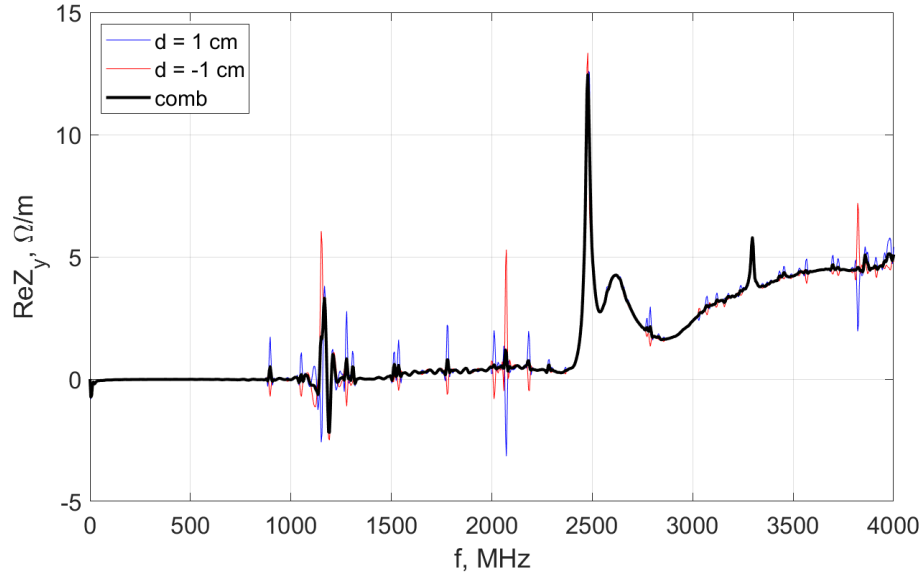


Figure 4: The real part of the vertical impedance: blue – $d_1 = 1$ cm, red – $d_2 = -1$ cm, black – Eq. (1).

In Fig. 4 the $\text{Re } Z_y$ calculated with $d_1 = 1$ cm and $d_2 = -1$ cm are slightly different, but mostly the curves overlap, except for some peaks. The same was observed when we used a different value for the second run, $d_2 = 2$ cm. It likely means that the section vertical asymmetry is insignificant, from the impedance viewpoint, due to a good screening of the vacuum plenum by the pumping grid. The resulting vertical impedance from Eq. (1) – the black curve in Fig. 4 – is practically the same for both choices of d_2 .

We plot both the real and imaginary parts of the vertical transverse impedance calculated using Eq. (1) in Fig. 5. The blue curve in Fig. 5 is the same as the black one in Fig. 4.

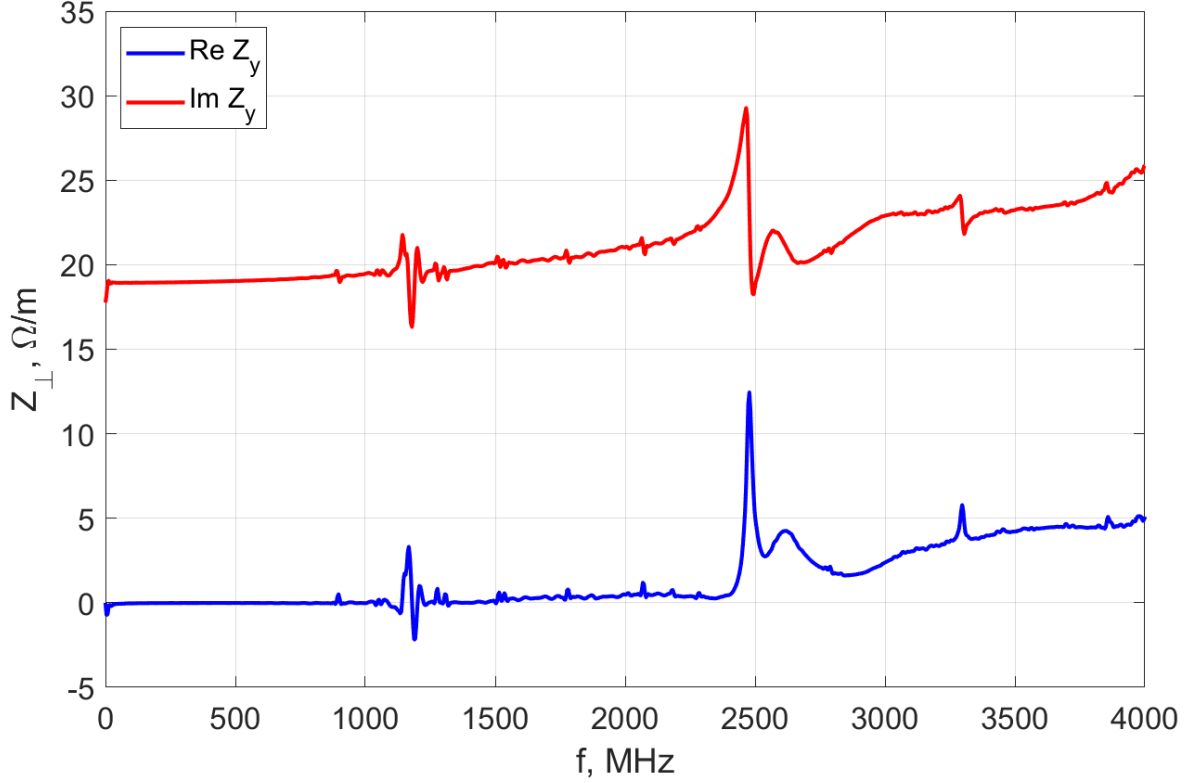


Figure 5: The vertical dipole impedance (blue – real part, red – imaginary part) of the inter-cell section, calculated from wake potentials, versus frequency.

The imaginary part of the vertical transverse impedance in Fig. 5 is nearly constant, about 19 Ω/m , while the real part is near zero, in the frequency range up to 1 GHz. One can notice one tiny peak at about 900 MHz, below the beam-pipe lowest cutoff frequency. It is likely related to a resonance mode in the vacuum plenum.

2.3. Resonances. From comparison of Fig. 5 and Fig. 3, one can see that the vertical impedance has more resonances than the horizontal one. This is expected since the vacuum plenum can introduce additional vertical resonances. However, many additional resonance peaks of the vertical impedance are rather small. Now we look at the lowest resonances of the transverse dipole impedance in the inter-cell section with CST eigensolver.

The calculated parameters of the lowest modes contributing to the vertical impedance are summarized in Table 2. The mode quality factors are calculated assuming stainless-steel SS304 walls with conductivity $\sigma = 1.43 \cdot 10^6$ Sm/m.

Table 2: Lowest vertical resonance modes of inter-cell section.

Mode	f , MHz	Q_{ss}	$R_{\perp y}$, Ω/m
1	891.9	3302	288
2	1050.4	4700	259
3	1150.1	950	280
4	1188.4	5998	$1.62 \cdot 10^{-3}$
5	1220.0	2261	97

The mode electric fields are shown in Figs. 6-7. The field normalization is the default for CST MicroWave Studio eigensolver: the total mode energy is 1 J.

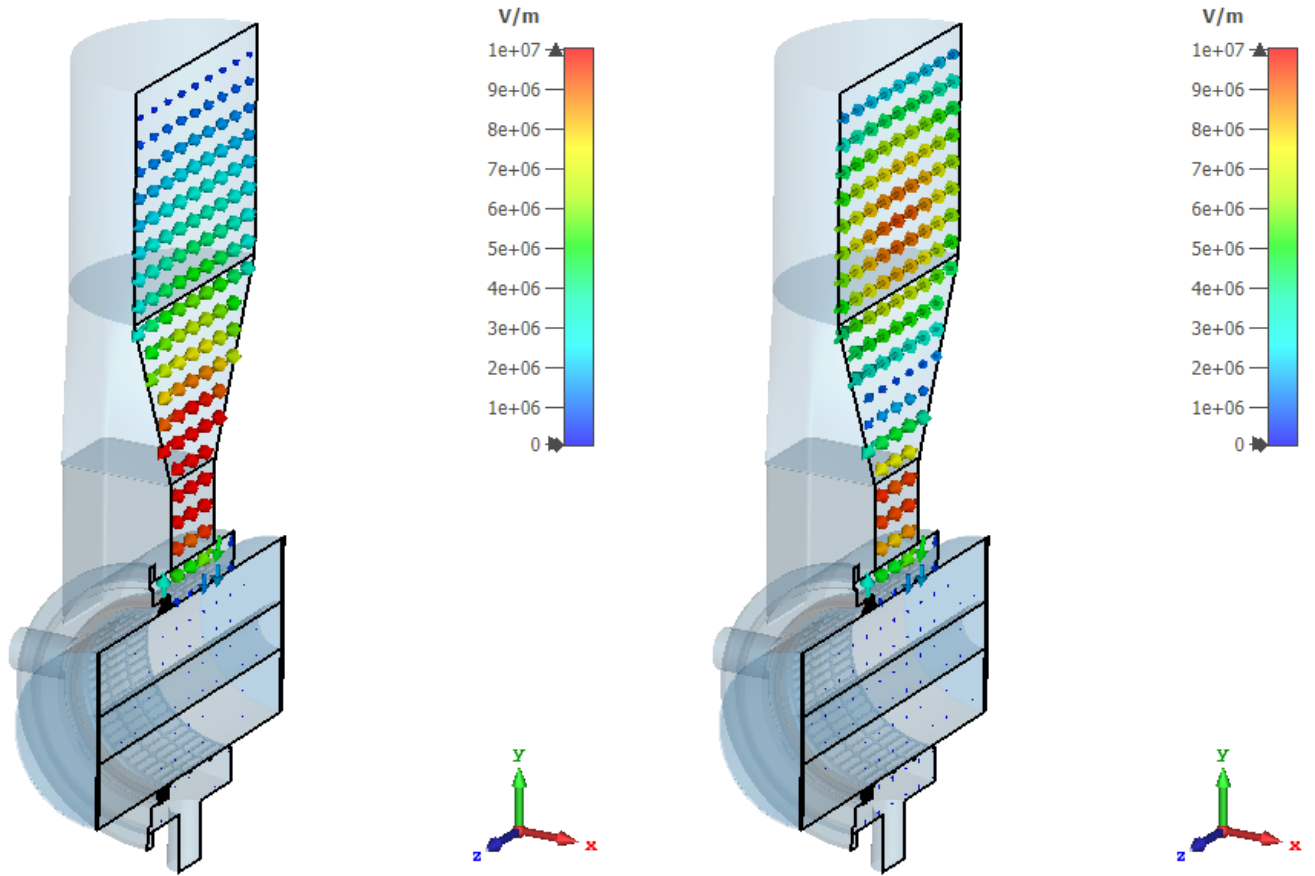


Figure 6: Electric fields of the first two lowest vertical modes in inter-cell section: left – mode 1 in Table 2 (892 MHz), right – mode 2 (1050 MHz).

Modes 1 and 2 in Fig. 6 are clearly vacuum-plenum modes, with half-wavelength and full wavelength along the duct. Their frequencies are defined mainly by the duct length; they can change when a vacuum pump is connected at the top. Here we assumed a flat metal surface on top.

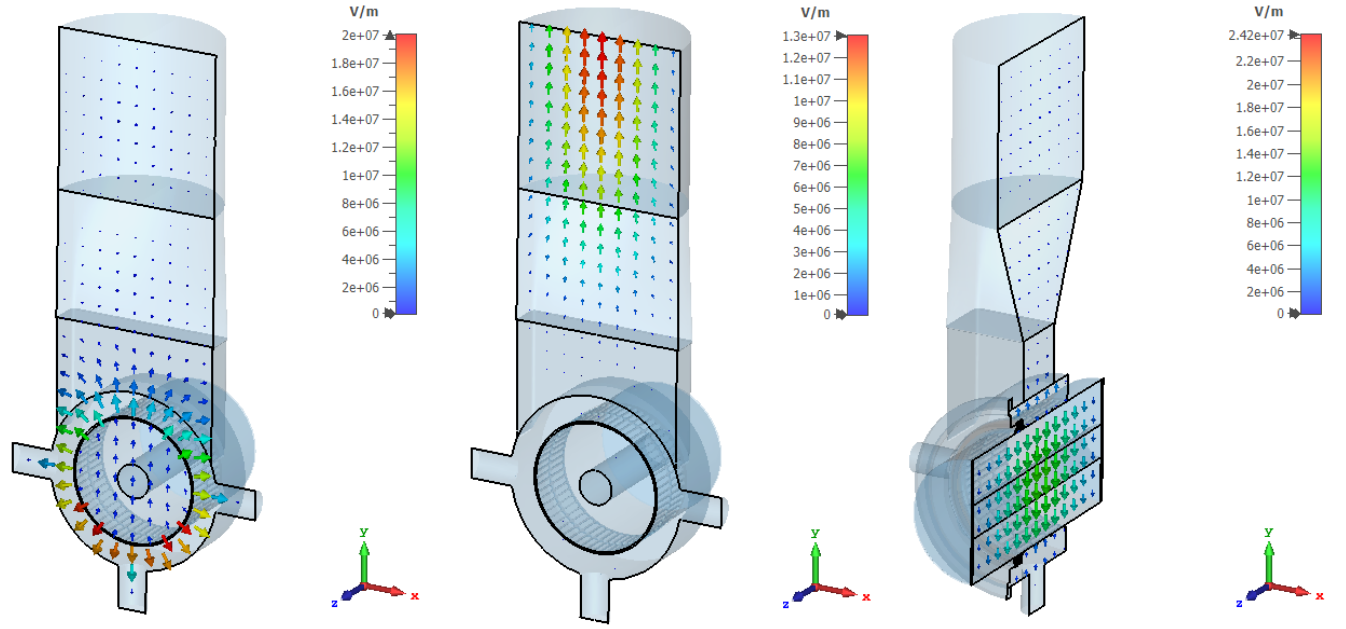


Figure 7: Electric fields of the next three vertical modes in inter-cell section: left – mode 3 in Table 2 (1150 MHz), center – mode 4 (1188 MHz), right – mode 5 (1220 MHz).

Mode 3 has a frequency slightly below the H-mode pipe cutoff frequency. From Fig. 7, this is a trapped mode due to slots in the pumping grid; cf. tech note [3]. Mode 4 has fields mainly in the outer part of the vacuum plenum and practically no fields in the beam pipe; this is why its coupling impedance is very low. The frequency of mode 5 is above the lowest cutoff frequency. This is a pipe mode; its exact frequency may depend on the length of pipe considered in computation. Clearly, for modes 3 and 5 the fields in the outer vacuum plenum are small compared to the fields in the pipe and grid regions.

The calculated parameters of the three lowest horizontal modes of the inter-cell section are summarized in Table 3. The mode electric fields are shown in Fig. 8.

Table 3: Lowest horizontal resonance modes of inter-cell section

Mode	f , MHz	Q_{ss}	$R_{\perp x}$, Ω/m
1	1044.0	5569	$2.3 \cdot 10^{-5}$
2	1212.3	1663	33.8
3	1249.7	1493	12.0

The first mode (Fig. 8, left) has very low fields in the pipe region, this is why its transverse impedance is very small. On the other hand, fields of mode 2 and 3 are mainly concentrated in the beam pipe and surrounding part of the vacuum plenum. These two modes likely correspond to the first peak of the horizontal dipole transverse impedance calculated from wakes in Fig. 3.

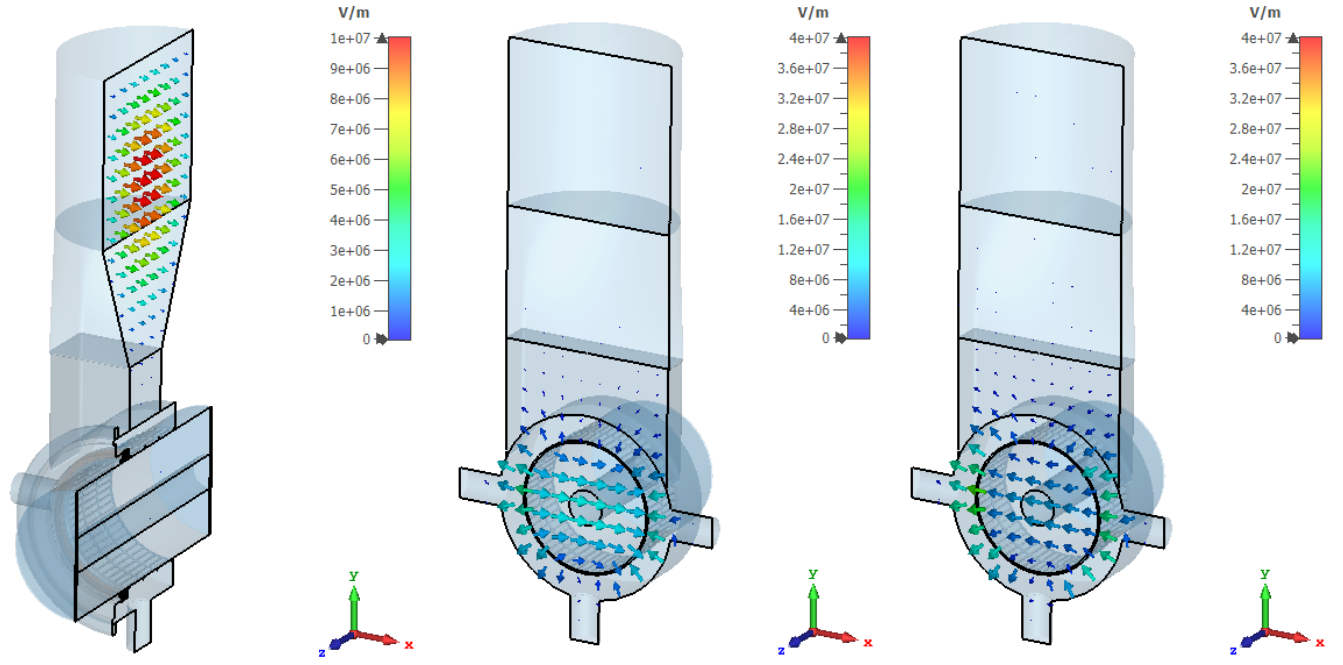


Figure 8: Electric fields of the three lowest horizontal modes in inter-cell section: left – mode 1 in Table 3 (1044 MHz); center – mode 2 (1212 MHz); right – mode 3 (1250 MHz).

2.4. High-frequency resonances. From transverse wake impedances in Figs. 3, 5 and the longitudinal wake impedances in Fig. 2, we can see that higher peaks are located near the cutoff frequencies: at about 1.2 GHz – TE_{11} cutoff; near 1.5 GHz – TM_{01} cutoff; and near 2.45 GHz – TM_{11} cutoff.

One can estimate the lowest frequencies of other potential high-frequency resonances using condition $\lambda/2 = l_c$, where l_c is a characteristic length of discontinuity. For slots in the pumping grid, the slot length is $l_{sl} = 30$ mm. The corresponding frequency $f_{sl} = c/(2l_{sl}) = 5$ GHz. For bellows, with typical length $l_b = 12.2$ mm, the expected resonances of this kind start at $f_b = c/(2l_b) = 12.3$ GHz. Both frequencies are much higher than the frequencies of concern for beam breakup. Resonances at such high frequencies are not considered important for the beam stability in induction linacs.

3. Summary.

In Sec. 2, the beam coupling impedances of the inter-cell section for the Scorpion linac are analyzed. The calculated impedances are typical for small discontinuities: they are inductive at low frequencies and have narrow resonances caused by trapped modes near the beam-pipe cutoff frequencies, which start at about 1.2 GHz. There are additional vertical resonances due to vacuum plenum below the cutoff, but they are rather weak due to good screening of the plenum by the slotted pumping grid.

Overall, the calculated transverse shunt impedance values for the inter-cell section are small. We can conclude that the inter-cell pumping section design is safe from the viewpoint of beam stability.

4. References.

1. S.S. Kurennoy, R.L. Gluckstern, and G.V. Stupakov. “Coupling impedances of small discontinuities: a general approach.” *Phys. Rev. E*, **52**, 4354 (1995).

2. S.S. Kurennoy. "Impedance of bellows in Scorpis linac." Tech note AOT-AE: 20-004 (TN), Los Alamos, NM, May 2020.
3. S.S. Kurennoy. "Impedances of vacuum pumping section in Scorpis linac." Tech note AOT-AE: 20-005 (TN), Los Alamos, NM, June 2020.
4. CST Studio Suite, 2020. www.cst.com
5. E. Colunga, A.K. Ortega, Private communications, July 2020.